Raman scattering experiments using microwaves in inductively coupled cool plasma

S. Casserly[1], K. Wilson[1], L. Selman[1], C.G. Whyte[1], A.D.R. Phelps[1], M.E. Koepke[1,2], R.A. Cairns[1,3], R. Bingham[1,4], B. Eliasson[1] D.C. Speirs[1], W. Strachan[1], C.W. Robertson[1], P. MacInnes[1], A.W. Cross[1], K. Ronald[1]

1. *SUPA and Department of Physics, University of Strathclyde, Glasgow, G4 0NG, Scotland, UK*
2. *Department of Physics, West Virginia University, Morgantown, WV 26506-6315, West Virginia, USA*
3. *School of Mathematics and Statistics, University of St. Andrews, St. Andrews, KY16 9SS, Scotland, UK*
4. *STFC Rutherford Appleton Laboratory, Harwell, OX11 0QX, England, UK*

Abstract

The linear plasma experiment at the University of Strathclyde was commissioned to investigate a range of microwave-plasma interactions using beat microwaves, including parametric interactions such as Raman scattering. Experiments to date have investigated beat-driven Raman scattering using high-power microwaves. Early numerical and experimental results presented here support theoretical predictions and show a strong coupling between the beat wave and Langmuir wave when their frequencies are well matched.

Introduction and theory

The study of microwave-plasma interactions is an increasingly important field of plasma physics, with relevance to several major applications. One notable example is microwave heating and current drive (HCD) methods used in magnetic confinement fusion, with STEP planning to solely use microwave (HCD) to achieve fusion conditions [1]. A particularly interesting class of microwave-plasma interactions is that of *parametric instabilities*: a three wave interaction in which a natural plasma mode grows while an incident pump wave decays [2]. Raman scattering is a parametric interaction in which an incident electromagnetic (EM) wave couples to an electrostatic (ES) electron oscillation ("Langmuir wave"). These two waves beat together to produce a scattered EM wave. The interaction is described by resonance conditions which capture conservation of energy and momentum:

$$\omega_0 = \omega_1 + \omega_L \tag{1}$$

$$\boldsymbol{k}_0 = \boldsymbol{k}_L + \boldsymbol{k}_1 \tag{2}$$

where ω_0 is the frequency of the incident EM wave, ω_L is the electron plasma frequency, and ω_1 is the frequency of the scattered EM wave (with the same convention applying to the wavevectors $\boldsymbol{k}$). For Raman scattering to occur, the frequency of the incident "pump" wave must satisfy $\omega_0 > 2\omega_L$, which corresponds to $n_e < \frac{1}{4}n_{crit}$, in terms of the electron density. Kruer finds the threshold intensity of the pump, a_0, can be expressed in terms of the plasma and pump wave parameters: [3]:

$$a_0 = \frac{2\nu_{ei}}{kc}\sqrt{\frac{\omega_L}{\omega_1}}. \tag{3}$$

where ν_{ei} is the electron-ion collisional frequency. We may also write

$$a_0 = \frac{v_{os}}{c} = \frac{\sqrt{2I_{pump}}e\lambda_{pump}}{2\pi c^2 m_e}\left(\frac{\mu_0}{\epsilon_0}\right)^{\frac{1}{4}} \tag{4}$$

where v_{os} is the electron quiver velocity due to the electric field of the pump wave.

Parametric interactions with a single pump are well documented in the literature and have been studied over a wide range of conditions, ranging from laser-plasma experiments, tokamak plasmas, ionospheric plasmas and many more. In this investigation, we study the case where the natural plasma wave - a Langmuir wave in this case - is instead driven by a beat wave, i.e. two counter-propagating carrier signals, rather than a single pump. Consider two carriers with frequencies ω_0 and ω_1, where $\omega_0 > \omega_1$. These frequencies may be chosen such that they satisfy the resonance condition Eq. 1, giving:

$$\omega_0 = \omega_1 + \omega_L \implies \omega_{beat} \simeq \omega_L. \tag{5}$$

Thus, a Langmuir wave is resonantly driven in the plasma by the beat wave, providing that the density requirement is satisfied. Given counter-propagating carriers with $\boldsymbol{k}_0 = -\boldsymbol{k}_1$, Eq. 2 dictates that the Langmuir wave travels in the same direction as the high frequency carrier. The Langmuir wave will then interact with the incident EM waves via the typical Raman mechanism, leading to the generation of EM sidebands. Scattering from each carrier will

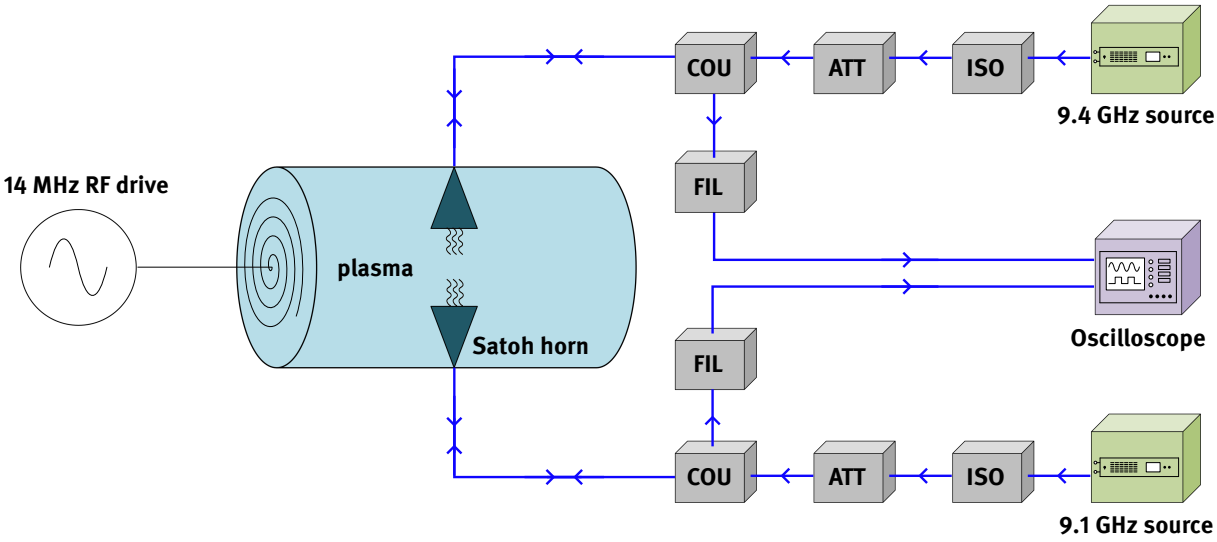

Fig. 1 Schematic of the experimental apparatus (not to scale), showing the RF drive system and antenna, and important components along the microwave arms. The Satoh horns are diametrically positioned on the lateral surface of the cylindrical vessel, in the cylinder's mid-plane. Blue lines and arrows indicate the path followed by the microwave signals.
ISO: ferrite isolator, ATT: attenuator, COU: directional coupler, FIL: analogue filter

produce four sidebands in total, but only two will be visible on a frequency spectrum as the anti-Stokes scatter from ω_1 and the Stokes scatter from ω_0 scatter into the other carrier signal. The two detectable sidebands are:

$$\text{Stokes from } \omega_1 : \ \omega_- = \omega_1 - \omega_L \text{anti-Stokes from } \omega_0 : \ \omega_+ = \omega_0 + \omega_L. \tag{6}$$

This article details the design of the linear plasma experiment at the University of Strathclyde. We also present early results from experiment and particle in cell (PiC) simulations investigating beat-driven Raman scattering in a cool, inductively coupled plasma.

Experimental apparatus

The Strathclyde plasma apparatus consists of a vacuum chamber $\sim$ 3 m long and $\sim$ 1 m in diameter which may be filled with gas at a desired pressure. This experiment uses He at 6.4 Pa. The RF drive system is connected to a flat spiral antenna with four turns, producing an inductively coupled plasma [4]. The power of the RF drive may be varied from 0 – 200 W. There are microwave arms on either side of the vacuum chamber, which are used to launch the beat wave and collect signals from the plasma. Signals at 9.1 GHz and 9.4 GHz are launched into the plasma volume as Gaussian beams via Satoh horns [5]. The low frequency carrier is produced by a travelling wave tube (TWT) amplifier at 7 kW, with $a_0 \sim 3 \times 10^{-4}$. The high frequency carrier is generated by a magnetron oscillator at 14 kW, with $a_0 \sim 6 \times 10^{-4}$. The beat wave duration is 1 μs, and has a frequency of 300 MHz. The output signal from the plasma volume in the direction of each carrier is collected, and time-domain waveforms are recorded. Fourier analysis is then employed to identify non-linear sidebands in the frequency domain. The key components of the experimental set-up are shown in Fig. 1.

The plasma conditions, namely electron density and temperature, are diagnosed using an RF-compensated Langmuir probe [6] [7], which accounts for the oscillation of the plasma potential at the RF drive frequency.

The bulk plasma is cool, with $T_e \sim 0.6$ eV. Fig. 2 shows electron density as a function of RF drive power for a range of gas pressures, while the probe tip was in the centre of the beat-wave plane between the two horn antennas. For a gas pressure of 6.4 Pa, the plasma density reaches and then exceeds 10^{15} m^{-3} for RF powers 70 – 100 W. In this regime, the Langmuir frequency will become similar to the beat frequency, meaning these are ideal plasma conditions for carrying out beat wave scattering experiments. For these parameters, the critical onset threshold defined in Eq. 3, 4 is $a_0 \sim 1 - 5 \times 10^{-5}$, meaning both microwave sources used are comfortably above this.

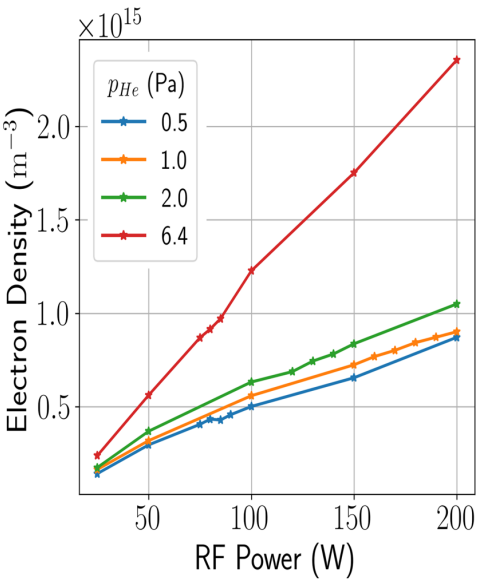

Fig. 2 RF power vs. electron density measurements

Beat-driven Raman scattering: experiment and PiC simulation

PiC simulations of this phenomenon were carried out using CST Studio 2026 [8]. Performing a PiC simulation of the total experimental plasma volume would be very computational expensive, even with modern GPU acceleration. Instead, a small representative cylinder is modelled with length 20 cm and radius 5 cm. The simulation was carried out for an electron density of 10^{15} m^{-3}, and carrier frequencies of 9.1 GHz and 9.4 GHz.

For these parameters, the Langmuir frequency is similar to the beat frequency. The simulation results corroborate the theoretical prediction outlined in the first section of this article. Fig. 3 shows a snapshot of the space-charge density profile of the plasma volume during the beat wave pulse, showing the driving of an electrostatic electron oscillation. Furthermore, analysis of the signals produced by the plasma in the simulation also show the generation of electromagnetic sidebands, at frequencies ω_- and ω_+ defined in Eq. 6. Consideration of the wavevectors of allowed scatterings indicates that the Stokes sideband at ω_- will propagate in the same direction as the high frequency carrier, and the anti-Stokes sideband at ω_+ will propagate in the same direction as the low frequency carrier. Such sidebands are visible in Fig. 4.

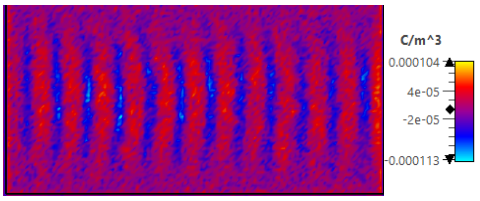

Fig. 3 Snapshot of space-charge density during the beat wave, from PiC simulation.

Experimental investigations were conducted over a wide range of plasma densities, and the strength of the non-linear sidebands measured. It is clear from Fig. 4 that the carrier signals are much stronger than the sidebands produced via the Raman interaction. This effect is enhanced in experiment by attenuators and filters which are needed to protect sensitive electronics from powerful microwave signals. To counteract this, several repeat waveforms are measured for a given RF drive power and an average spectrum with improved signal to noise ratio is determined. The weak anti-Stokes signal is still difficult to see, and so analysis focusses on the stronger Stokes sideband. As RF power increases, plasma density increases as shown in Fig. 2. At an RF power in the range $\sim$ 70 – 100 W, Eq. 5 will be satisfied as $\omega_L \rightarrow \omega_{beat}$, and we may say the plasma is *in resonance* with the beat wave. At this plasma density, the beat wave and Langmuir wave are resonantly coupled and will produce a strong Stokes sideband. Fig. 5 shows the Stokes sideband amplitude in both carrier directions for a range of plasma densities. It is clear that when the resonance conditions are fulfilled, there is a marked uplift in sideband strength. It is also noted that the Stokes sideband is much stronger in the direction of the high frequency carrier.

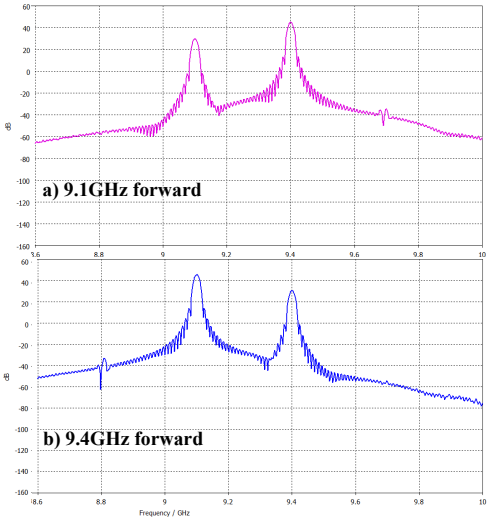

Fig. 4 Frequency spectra from PiC simulations, in both carrier directions.

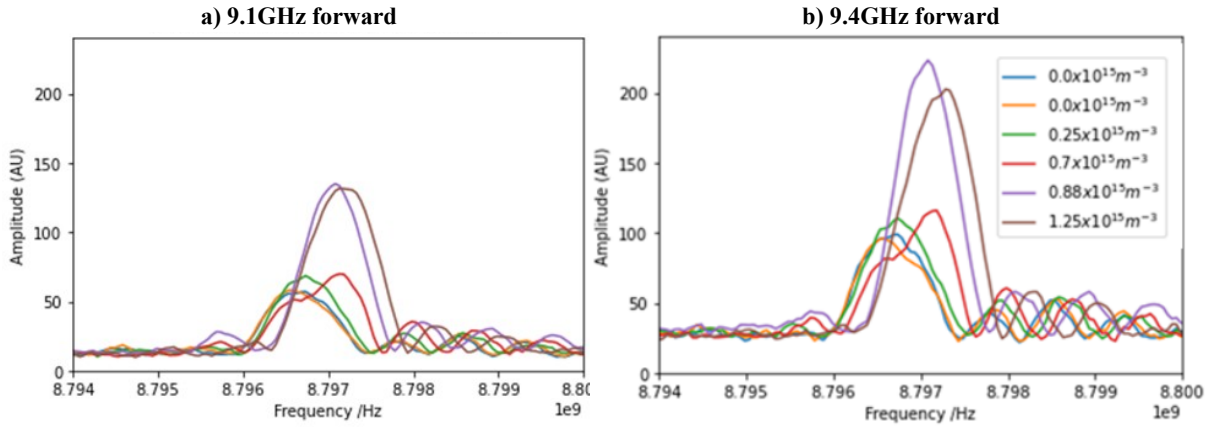

Fig. 5 Experimentally determined spectra for a range of plasma densities, showing the Stokes sideband amplitude in both carrier directions.

The non-zero amplitude of the sidebands for low plasma densities may be explained by the use of “ferrite isolators" in the microwave arms of the apparatus. They are employed to prevent reflected signals from travelling back into the microwave sources. These devices exhibit non-linear properties when high-power microwaves travel through them. When two signals pass through the junction, a process known as “third order intermodulation distortion" (IMD) generates unwanted signals [9]. In this experiment, the frequencies of these signals coincides with the frequencies of the sidebands produced via the Raman interaction. This means there is a systematic “apparatus contribution" to the EM sidebands which has to be taken into account.

Summary and Future Work

The linear plasma apparatus used in this experiment was commissioned with microwave-plasma interactions in mind. As a result, it is able to access a wide range of plasma conditions which are well suited to these studies. Plasma densities $\sim 10^{15}$ m^{-3}, corresponding to $\omega_L \sim 300$ MHz, are achievable for a modest RF power and provide ideal conditions for experiments with the available microwave apparatus.

The results of numerical and experimental studies conducted to date support the theoretical prediction that a beat-driven Raman scattering occurs when the resonance conditions are satisfied, producing a Langmuir wave in the plasma and electromagnetic sidebands. Investigations are ongoing, with plans to characterise the temporal and spatial growth of the interaction, as well as the dependence of the Stokes sideband on carrier signal amplitude. Several hardware upgrades are planned which will facilitate further experiments, including lenses which will increase carrier intensity and minimise spurious resonances and scatters within the vacuum vessel. In addition, the magnetron oscillator will be replaced by a second TWT amplifier, allowing for the beat wave duration to be significantly increased. Further analytical and numerical studies will also be conducted to enhance our understanding of this phenomenon.

The linear plasma apparatus at the University of Strathclyde also has the capability to operate in the helicon mode, which has not been discussed in this article. Currently, two electromagnet coils are installed and four more are ready to be mounted. With all six coils in use, approximately 2 m of the length of the vessel will be magnetised, with field strength 0.875 T. The ability to produce both magnetised and field-free plasmas significantly broadens the horizon of possible interactions which may be studies using this apparatus. Similar experiments using beat microwaves may be conducted as part of the wider project which focus on other fundamental plasma resonances, such as electron and ion cyclotron resonances, and upper hybrid plasma oscillations.

Acknowledgements

The authors thank the Engineering and Physical Sciences Research Council (EPSRC), Energy Transfer Technologies Doctoral Training Hub, and MBDA (UK) Ltd. for supporting this work through grants EP/Y029240/1 and EP/R004773/1. We also thank MBDA (UK) Ltd. and TMD Technologies Ltd. for their generous industrial support.

References

[1] S. Freethy, L. Figini, S. Craig, M. Henderson, R. Sharma, T. Wilson, and the STEP team, “The optimisation of the STEP electron cyclotron current drive concept,” *Nuclear Fusion*, vol. 64, no. 12, 2024.

[2] T. J. M. Boyd and J. J. Sanderson, *The physics of plasmas / [internet resource]*. Cambridge, UK ; New York: Cambridge University Press, 2003.

[3] W. L. Kruer, *The physics of laser plasma interactions*. Frontiers in physics, Boulder, Colo. ; Oxford: Westview, 2003.

[4] P. Chabert, T. V. Tsankov, and U. Czarnetzki, “Foundations of capacitive and inductive radio-frequency discharges,” *Plasma Sources Science and Technology*, vol. 30, no. 2, 2021.

[5] A. D. Olver, P. J. B. Clarricoats, and K. Raghavan, “Dielectric cone loaded horn antennas,” vol. 135, no. 3, 1988.

[6] I. D. Sudit and F. F. Chen, “RF compensated probes for high-density discharges,” *Plasma Sources Science Technology*, vol. 3, no. 2, 1994.

[7] K. Wilson, *Development of a large RF plasma source for non-linear microwave-plasma interactions*. PhD thesis, University of Strathclyde, 2024.

[8] “CST Studio Suite 2026 Help | PIC Solver Overview.” `https://www.3ds.com/products/simulia/cst-studio-suite/electromagnetic-simulation-solvers`. Accessed on: 23/06/2026.

[9] P. Lui, “Passive intermodulation interference in communication systems,” *Electronics Communication Engineering Journal*, vol. 2, pp. 109–118, 1990.